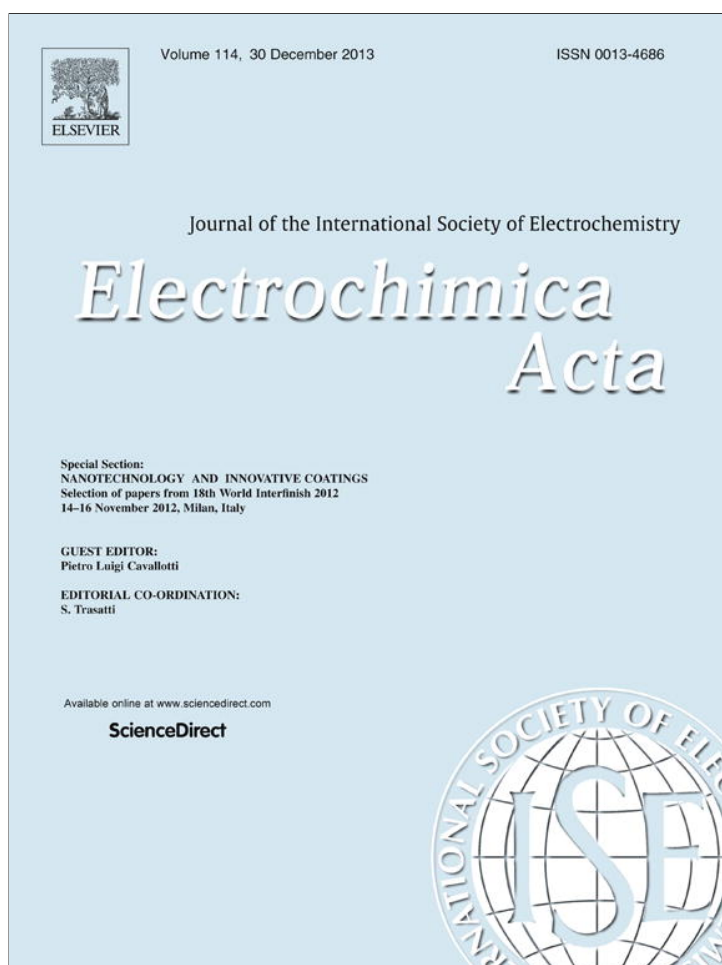


Provided for non-commercial research and education use.
Not for reproduction, distribution or commercial use.



This article appeared in a journal published by Elsevier. The attached copy is furnished to the author for internal non-commercial research and education use, including for instruction at the authors institution and sharing with colleagues.

Other uses, including reproduction and distribution, or selling or licensing copies, or posting to personal, institutional or third party websites are prohibited.

In most cases authors are permitted to post their version of the article (e.g. in Word or Tex form) to their personal website or institutional repository. Authors requiring further information regarding Elsevier's archiving and manuscript policies are encouraged to visit:

<http://www.elsevier.com/authorsrights>



Contents lists available at ScienceDirect

Electrochimica Acta

journal homepage: www.elsevier.com/locate/electacta

Hydrogen permeation through steel electroplated with Zn or Zn–Cr coatings

Tz. Boiadjieva^{a,*}, L. Mirkova^b, H. Kronberger^c, T. Steck^d, M. Monev^b^a Centre of Electrochemical Surface Technology GmbH, Viktor-Kaplan-Straße 2, 2700 Wiener Neustadt, Austria^b Institute of Physical Chemistry, Bulgarian Academy of Sciences, Acad. G. Bonchev Street, bl. 11, 1113 Sofia, Bulgaria^c TU-Vienna, Institute for Chemical Technology and Analytics, Getreidemarkt 9/164ec, A-1060 Vienna, Austria^d voestalpine Stahl GmbH, Voestalpine-Strasse 3, 4031 Linz, Austria

ARTICLE INFO

Article history:

Received 6 March 2013

Received in revised form 7 June 2013

Accepted 7 June 2013

Available online 15 June 2013

Keywords:

Electrodeposition

Zn and Zn–Cr alloy coatings

Hydrogen permeation

Devanathan–cell

ABSTRACT

Hydrogen permeation characteristics with steel samples, already electroplated with Zn or Zn–Cr are obtained. Alloy coatings with a thickness of 2.5 and 5.0 μm and various Cr content (3, 5 and 10 mass%) were prepared at conditions, close to industrial line trials. The investigations are performed in a conventional Devanathan–Stachurski cell in 0.5 M Na_2SO_4 solution, pH 6 at two current densities (30 and 300 mA cm^{-2}). The Zn and Zn–Cr coatings are impermeable during hydrogenation at a low charging current density and they permeate small amounts of hydrogen when a high charging current density is applied. The amount of hydrogen permeating into the steel substrate is in orders of magnitude lower in comparison to a bare steel substrate. Therefore, Zn and Zn–Cr coatings protect steel effectively under conditions which cause hydrogen ingress. The influence of the thickness of the Zn and Zn–Cr coatings as well as the influence of the Cr content in the Zn–Cr alloy on the hydrogenation of the steel substrate is expressed by negligible differences in the hydrogen permeation rates. The hydrogen permeation through Zn and Zn–Cr coatings is not a continuous process. Fluctuations of the permeation current which could be associated with the specific dynamics of hydrogen bubbles at the cathode surface and with the catalytic and barrier properties of the alloy coatings, regarding hydrogen evolution and permeation are registered. More expressed fluctuations of the permeation current are recorded in the case of the Zn–Cr alloy. During the charging of the Zn or Zn–Cr coatings at a high current density permanent structural changes occur. Disintegration of a subsurface metal layer and oxidation of the Zn coatings is observed, accompanied by crack formation in the case of Zn–Cr alloys.

© 2013 Elsevier Ltd. All rights reserved.

1. Introduction

It has been proved in the last 20 years that enhancement of the protective properties of Zn coatings to steel at a reduced layer thickness can be achieved by alloying Zn with the so-called *d*-block metals (Ni, Co, and Fe) [1]. By fulfilling the high requirements for corrosion protective metallic coatings as well as by showing very promising results in respect to joinability (spot weldability, laser weldability, and adhesive bondability), forming capability (coating adhesion, powdering, and friction behaviour), the Zn–Cr alloys turned out to be an attractive candidate for an industrial scale trail and further application in the automotive industry [2].

An important aspect of the electroplating process is the avoidance of hydrogen embrittlement of the steel substrate. Moreover,

it is of importance that already incorporated hydrogen in the substrate/coating system is enabled to conversely diffuse after deposition, during the stay or following thermal treatment of the coating. In the first part of this work, the hydrogen permeation process into the steel substrate during Zn–Cr electroplating was evaluated and compared to that of Zn [3]. The study of the hydrogen permeation into steel, already modified by the electrodeposited coatings is of practical and scientific interest, because of several reasons. The strongest hydrogenation of the steel substrate during Zn and Zn alloy deposition occurs in the initial stages of the electrocrystallization due to the lower hydrogen overvoltage on steel in comparison to that on Zn [4,5]. However, evolution, absorption and permeation of hydrogen also proceed during the formation of the metallic layer. Two hypotheses are proposed to explain the hydrogen embrittlement of steel [6]. The one hypothesis is the absorption of hydrogen by the steel before formation of the first Zn crystallites, and the other hypothesis is the trapping of hydrogen in the deposit during plating and subsequent diffusion of hydrogen in the steel.

* Corresponding author. Tel.: +43 1 58801 15879; fax: +43 1 58801 15899.

E-mail address: tzvetanka.boiadjieva@cest.at (Tz. Boiadjieva).

In the literature, few papers are devoted to studies of hydrogen permeation during cathode charging of steel, electroplated with a metallic coating: Zn–Ni [7–9], Zn–Ni or Zn–Ni–Cd [9,10], Zn–Co [11], and Zn–SiO₂ [12]. The results reveal higher hydrogen permeability of the alloys and of the composite deposits in comparison to that of pure Zn coatings.

In this part of the work, hydrogen permeation characteristics are obtained with steel samples, already electroplated with Zn or Zn–Cr in order to elucidate the hydrogen permeability of the coatings. The layers were produced at conditions, close to industrial line trials and with different thickness and Cr content.

2. Experimental

Zn–Cr alloy coatings with Cr content of 3, 5 and 10 mass% were electrodeposited in a 201 flow cell from an electrolyte, containing 40 g l⁻¹ Zn, 15 g l⁻¹ Cr (added as sulphates) and polyethyleneglycol with a mass of 6000 (PEG 6000) 1 g l⁻¹, pH 2.0 adjusted with sulphuric acid solution, at a flow rate of 4 m s⁻¹, current density between 80 and 120 A dm⁻² and an electrolyte temperature of 55 °C. The coatings were deposited onto mild steel substrates, mass%: C-0.12, Mn-0.6, P-0.045, S-0.045 (Metall-Folien GmbH, Main, Germany) with a thickness of 50 μm and a surface of 90 cm². The Zn–Cr coatings are having thickness of 2.5 and 5.0 μm. For comparison, Zn coatings with thickness of 2.5, 5.0 and 7.5 μm were electrodeposited from a pure Zn-electrolyte (without Cr(III) and PEG 6000).

The electrochemical technique of Devanathan–Stachurski [13] was used for studying hydrogen permeation into steel, electroplated with Zn or Zn–Cr coatings. In detail, the description of the hydrogen permeation measurements was given in a recent paper [3]. When bare steel sheet (St), steel, coated with Zn (St/Zn) or steel, coated with Zn–Cr (St/Zn–Cr) were subjected to hydrogen permeation measurements, the samples were mounted between both cells in such a way that a working surface of 1 cm² was exposed to the electrolytes with the Zn or Zn–Cr coating at the entry side of the steel membrane forming a bipolar electrode. The exit side of the membrane was preliminary electroplated with a thin (0.5 μm) Pd layer. 1 M NaOH solution was introduced into the output cell and a constant positive potential of 0.28 V/Hg/HgO was applied on the exit side of the membrane for a sufficiently long time to get a residual anodic current density below 1 μA cm⁻². Then, the input cell was filled with 0.5 M Na₂SO₄ solution, pH 6 and a current density (j_1) of 30 or 300 mA cm⁻² was applied at the entry face of the steel membrane. Previous studies on the hydrogen permeation process into the steel substrate during Zn–Cr electroplating were performed at a current density of 300 mA cm⁻² because of the specificity of the deposition process: Cr co-deposition with Zn starts at a current density higher than 200 mA cm⁻² [14]. The ionization current j_2 at the exit side, a direct measure of the hydrogen permeation rate in the metal, was recorded against time. In the graphs, the corresponding transients $j_2(t)$ after a subtraction of the residual anodic current density are presented.

Experiments in aerated and de-aerated 0.5 M Na₂SO₄ solution, pH 6 were performed aiming to evaluate the effect of oxygen in the electrolyte used for hydrogen permeation studies. For the removal of oxygen the electrolyte was de-aerated with Ar for 1 h and then transferred to the input cell.

In order to examine the morphology of the coatings before and after the experiments with the Devanathan–Stachurski hydrogen permeation technique, a XL 30 environmental scanning electron microscope (ESEM) with field emission gun (FEI Co., Netherlands) was used. The elemental composition was measured by Energy

Dispersive X-Ray (EDX) spectrometer supported with Genesis software (USA).

3. Results and discussion

3.1. Hydrogen permeation during polarization of steel

First, as a basis for further evaluation and comparison with coated samples, bare steel membranes were polarized in aerated 0.5 M Na₂SO₄ solution. The hydrogen permeation transients, obtained at a charging current density $j_1 = 30$ mA cm⁻² or 300 mA cm⁻² are shown in Fig. 1.

A short delay is observed at the very beginning of both transients. The hydrogen permeation in mild steel, similarly to α-iron is not controlled by hydrogen diffusion, therefore, the delays of the transients can be related to slower surface processes affecting the hydrogen entry and/or by hydrogen trapping affecting the hydrogen transport [15,16].

In the case of the lower polarization of the steel membrane at 30 mA cm⁻², a value of about 30 μA cm⁻² is measured for the steady state hydrogen permeation rate. At the higher polarization of the steel membrane (300 mA cm⁻²), two stages are observed on the permeation transient: a traditional sigmoid shape of the curve with a steady state value of about 30 μA cm⁻² in the first 25 min from the beginning of polarization, and a very sharp increase of the hydrogen permeation rate in the second part of the curve. The comparison of the transient obtained at 30 mA cm⁻² and the first

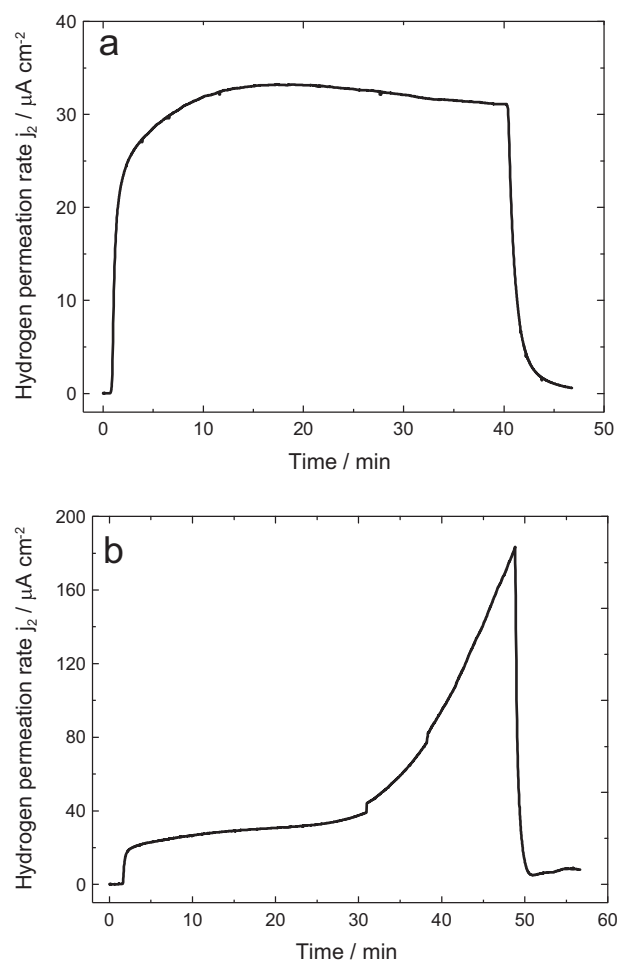


Fig. 1. Permeation transients, measured during polarization of St in 0.5 M Na₂SO₄ solution, pH 6 at $j_1 = 30$ mA cm⁻² (a) and at $j_1 = 300$ mA cm⁻² (b).

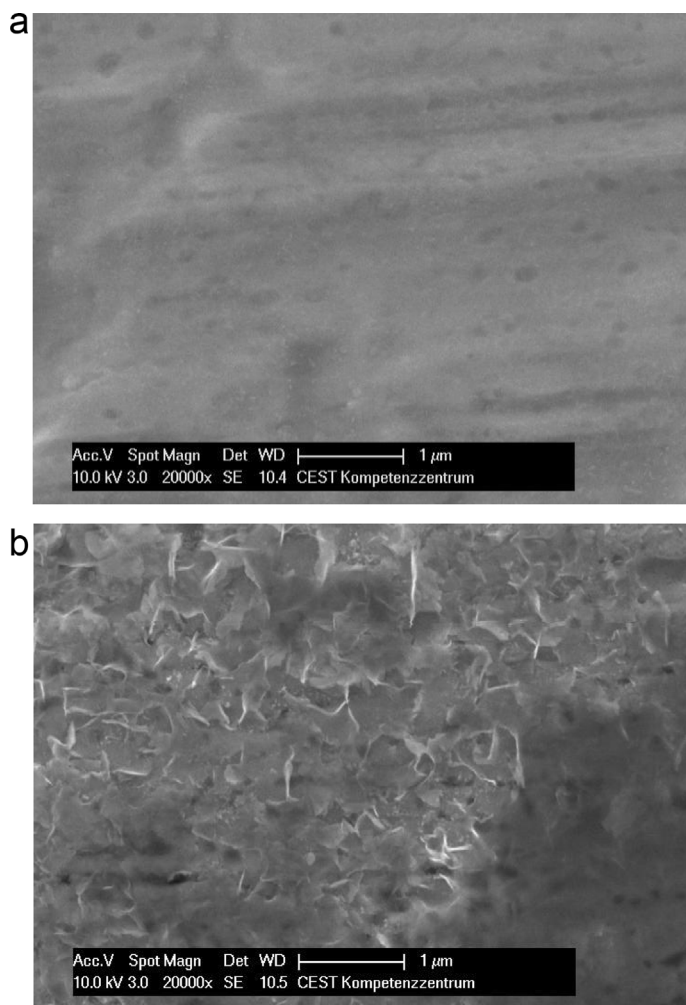


Fig. 2. SEM images of St before (a) and after (b) 50 min polarization at $j_1 = 300 \text{ mA cm}^{-2}$ in 0.5 M Na_2SO_4 solution, pH 6.

stage of the transient, obtained at 300 mA cm^{-2} shows nearly similar steady state values of the hydrogen permeation rate, which reveals that the value of the charging current density 30 mA cm^{-2} is sufficiently high in order to ensure saturation of the steel surface with adsorbed hydrogen atoms. The strong increase of the hydrogen permeation rate in the second part of the curve, obtained at the higher charging current density of 300 mA cm^{-2} can be explained by alterations of the surface and the subsurface of the steel membrane when it is subjected to the influence of the strong hydrogen flow (Fig. 2).

These results are similar to those obtained during cathode charging of steel in 0.5 M Na_2SO_4 solution with a lower value of pH [3]. The high charging current density, also in this case leads to drastic cathode polarization and of course to intensive hydrogen evolution. The alkalization in the vicinity of the electrode surface points to the conclusion made by Zakroczyński et al, that a long charging of Fe in alkaline medium causes disintegration of a subsurface metal layer and, as result, the metal surface became more prone to both hydrogen absorption and corrosion [15,17].

Moreover, X-ray microanalysis of the steel membrane after 50 min polarization at $j_1 = 300 \text{ mA cm}^{-2}$ shows presence of Na (Fig. 3), probably as a result of the incorporation of the alkali metal into the electrode. Thus, a contribution of Na to the observed structural changes, related to loosening and destroying of the metal could be considered, as well [18].

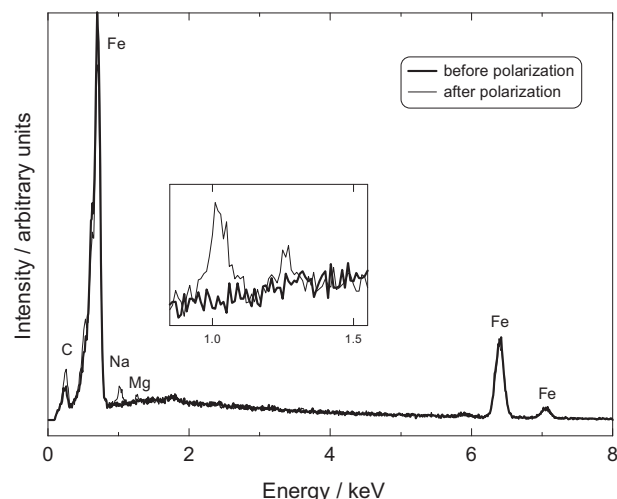


Fig. 3. X-ray microanalysis of St before and after 50 min polarization at $j_1 = 300 \text{ mA cm}^{-2}$ in 0.5 M Na_2SO_4 solution, pH 6.

3.2. Hydrogen permeation during polarization of steel, electroplated with Zn coating

The permeation transients, obtained during charging of steel, covered with electrodeposited Zn coatings (St/Zn) with a thickness of 2.5, 5.0 or 7.5 μm are presented in Fig. 4.

Very low, wide maxima at the beginning of all transients and a consequent decrease of the hydrogen permeation rate till low values of the steady state are observed. The highest maximum and the highest steady state permeation rate are registered in the case of the thinnest Zn coating (2.5 μm), probably due to the small thickness and higher porosity of the layer. The results are in correlation with data from previous studies on hydrogen evolution on Zn, showing the influence of the steel substrate on the electrochemical performance of electrodeposited Zn 2.5 μm coatings. The hydrogen permeation transients of steel, electroplated with Zn coatings with a thickness of 5 or 7.5 μm are nearly similar. Therefore, the increase of the thickness of the Zn coating over 5 μm does not lead to stronger inhibition of the hydrogen permeation into the steel substrate. Fig. 4b demonstrates the common shape of the permeation transients, which cannot be distinguished in Fig. 4a.

The comparison of Figs. 1b and 4 reveals that even the thinnest Zn coatings tested play the role of an effective barrier for the hydrogen permeation into the steel substrate, although the very intensive hydrogen evolution on the Zn coatings. This conclusion is in agreement with the results of other authors. It has been shown by Paatsch that after the build up of Zn layer with a thickness of about 0.5 μm, no hydrogen permeation is registered [4].

In order to evaluate the influence of the charging current density, samples of St/Zn 2.5 μm were subjected to hydrogenation at a low current density of the charging current (30 mA cm^{-2}) during 20 min and thereafter, in the same experiment, a charging current density of 300 mA cm^{-2} was applied (Fig. 5).

In the case of the low charging current, no hydrogen penetration into the steel substrate is registered. The hydrogen permeation rate does not exceed the value of the residual current of about $0.5 \mu\text{A cm}^{-2}$, in contrast, it continues to decrease. This course of the curve can be related to a flow of hydrogen, remaining in the system substrate/coating after deposition and pre-treatment. When the charging current of 300 mA cm^{-2} is applied, the transient shows an initial sharp maximum, followed by a stable steady state permeation rate. However, even in the case of the high charging current, the maximal and the steady state values of the permeation rate are

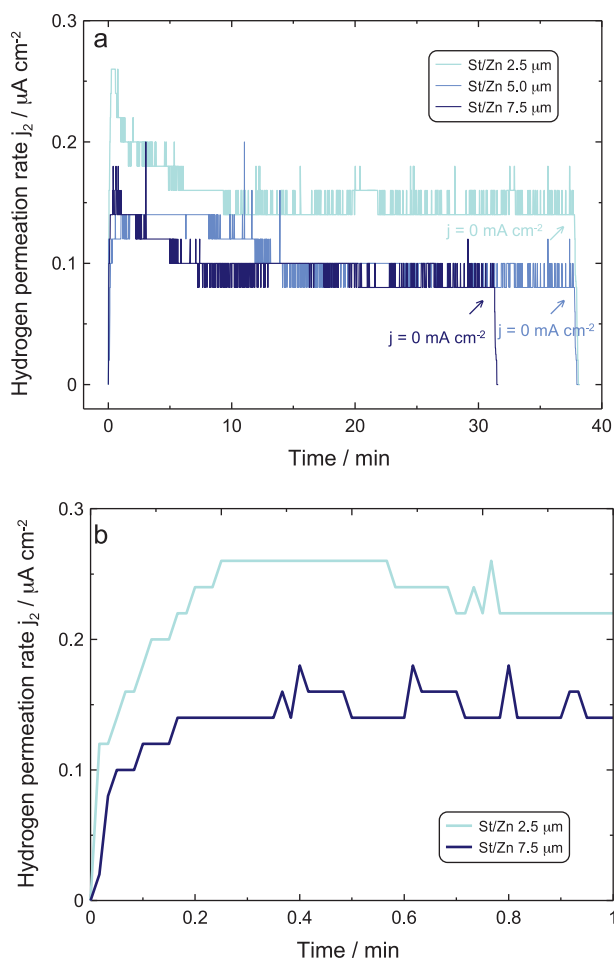


Fig. 4. Permeation transients measured during polarization of St/Zn with various thickness of the Zn coatings at $j_1 = 300 \text{ mA cm}^{-2}$ in $0.5 \text{ M Na}_2\text{SO}_4$ solution, pH 6 with different time resolution: 40 min (a) and 1 min (b).

very low, similarly to those shown in Fig. 4. Thereby, these results confirm the conclusion that the Zn coatings exert strong inhibition of the hydrogen penetration into the steel substrate. It is known that Zn is a metal with high hydrogen overvoltage and is unable to adsorb and absorb hydrogen atoms to any great extent, because

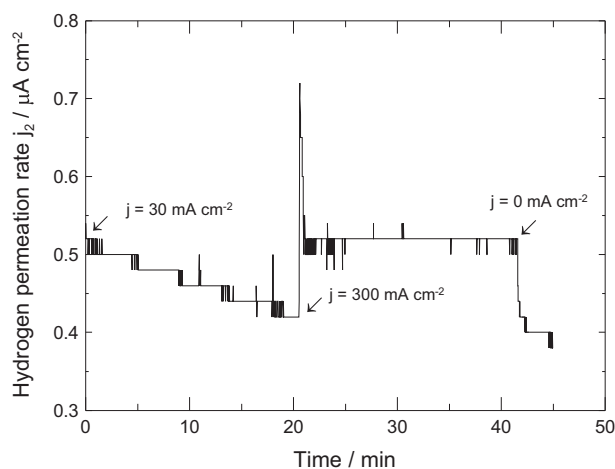


Fig. 5. Permeation transients, measured during subsequent polarization of St/Zn $2.5 \mu\text{m}$ at $j_1 = 30$ and 300 mA cm^{-2} in $0.5 \text{ M Na}_2\text{SO}_4$ solution, pH 6. (The curve in the figure starts from the residual anodic current density.)

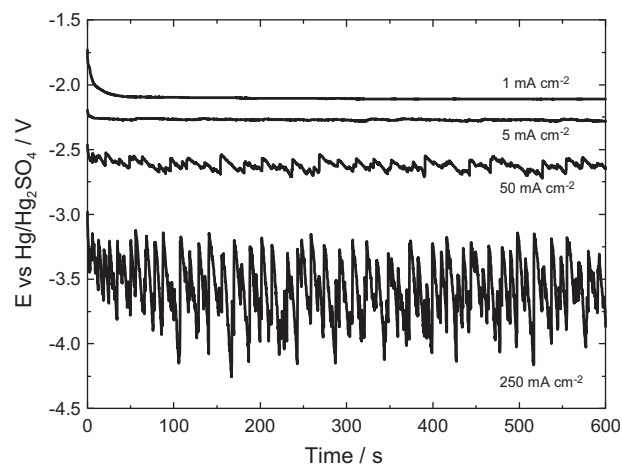


Fig. 6. Galvanostatic potential vs. time curves for Zn $7.5 \mu\text{m}$ in $0.5 \text{ M Na}_2\text{SO}_4$ solution, pH 6 measured at different current density.

of weak interaction with hydrogen and low hydrogen absorption capability of the close-packed hexagonal structure. In this regard, the hydrogen permeation recorded at the higher current density (300 mA cm^{-2}) could be explained by assuming that above a certain hydrogen pressure, hydrogen permeates through defects in the Zn layer.

In order to evaluate the polarization conditions at the electrode surface, potential-time curves in galvanostatic conditions were recorded (Fig. 6). The increase of the current density causes steep raise of the overvoltage and potential oscillations. The potential oscillations result from hydrogen gas bubbles, which grow and partially block a part of the cathode surface. Under constant current polarization, the real cathode current density and the overpotential of the hydrogen evolution reaction (HER) increase. When hydrogen bubbles break away, the cathode surface suddenly increases, the real current density decreases, and the overpotential of the HER decreases.

Similarly to the steel, after the permeation experiments changes in the morphology of the Zn coatings are observed. For example, the SEM image of the surface of Zn $5 \mu\text{m}$ before polarization (Fig. 7a and b) shows a uniform structure of the Zn coating with a hexagonal shape of the crystal grains. Upon the influence of the intensive hydrogen flow during the polarization at 300 mA cm^{-2} considerable changes of the surface structure of the Zn coating are caused (Fig. 7c). Besides, EDX analyses showed a higher content of O on the surface of the polarized coating in the order of one magnitude and the X-ray diffraction pattern indicated the presence of ZnO.

3.3. Hydrogen permeation during polarization of steel, electroplated with Zn–Cr coating

This section of the paper presents the influence of the thickness of the Zn–Cr coatings (2.5 and $5.0 \mu\text{m}$), the influence of the coating's composition (3, 5 and 10% Cr) as well as the influence of the charging current density (30 or 300 mA cm^{-2}) on the hydrogen permeability of the St/Zn–Cr system.

The hydrogen permeation transients of St/Zn–Cr $2.5 \mu\text{m}$ and St/Zn–Cr $5 \mu\text{m}$ are shown in Fig. 8. The shape of the transients is similar with that of the transients, obtained with St/Zn system. It is characterized by a maximum at the beginning of the transient, followed by a decrease of the hydrogen permeation rate until a steady state. The values of the maximal and steady state permeation rates of the transients of St/Zn–Cr are very low and similar to those measured with St/Zn. It can be seen that more fluctuations of the permeation current are registered in the case of St/Zn–Cr.

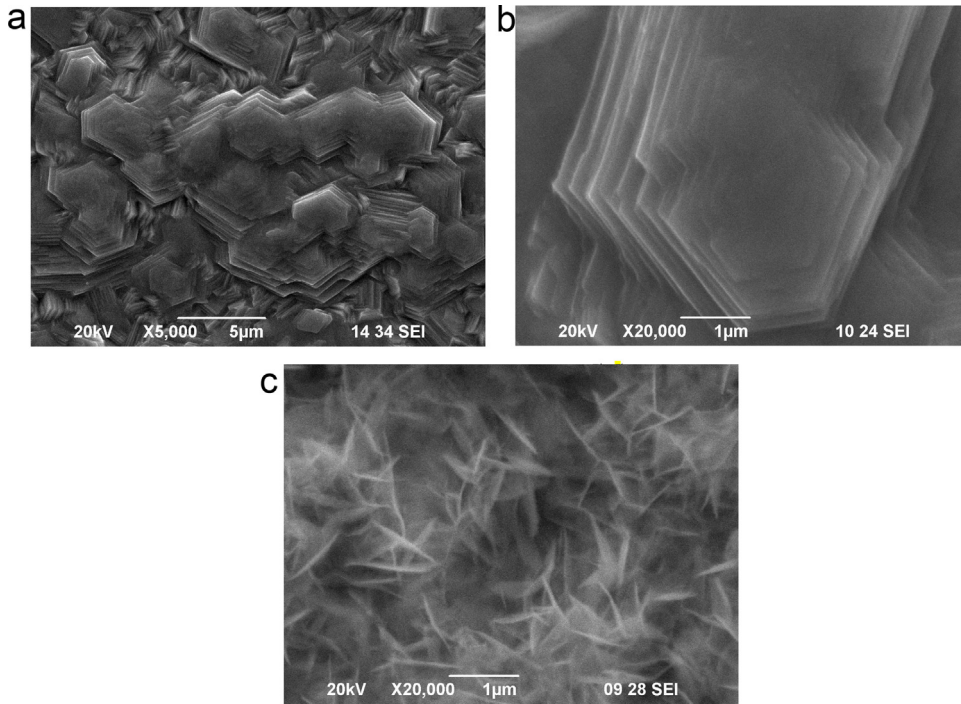


Fig. 7. SEM images of Zn 5 μm before (a and b) and after (c) polarization at $j_1 = 300 \text{ mA cm}^{-2}$ in 0.5 M Na_2SO_4 solution, pH 6.

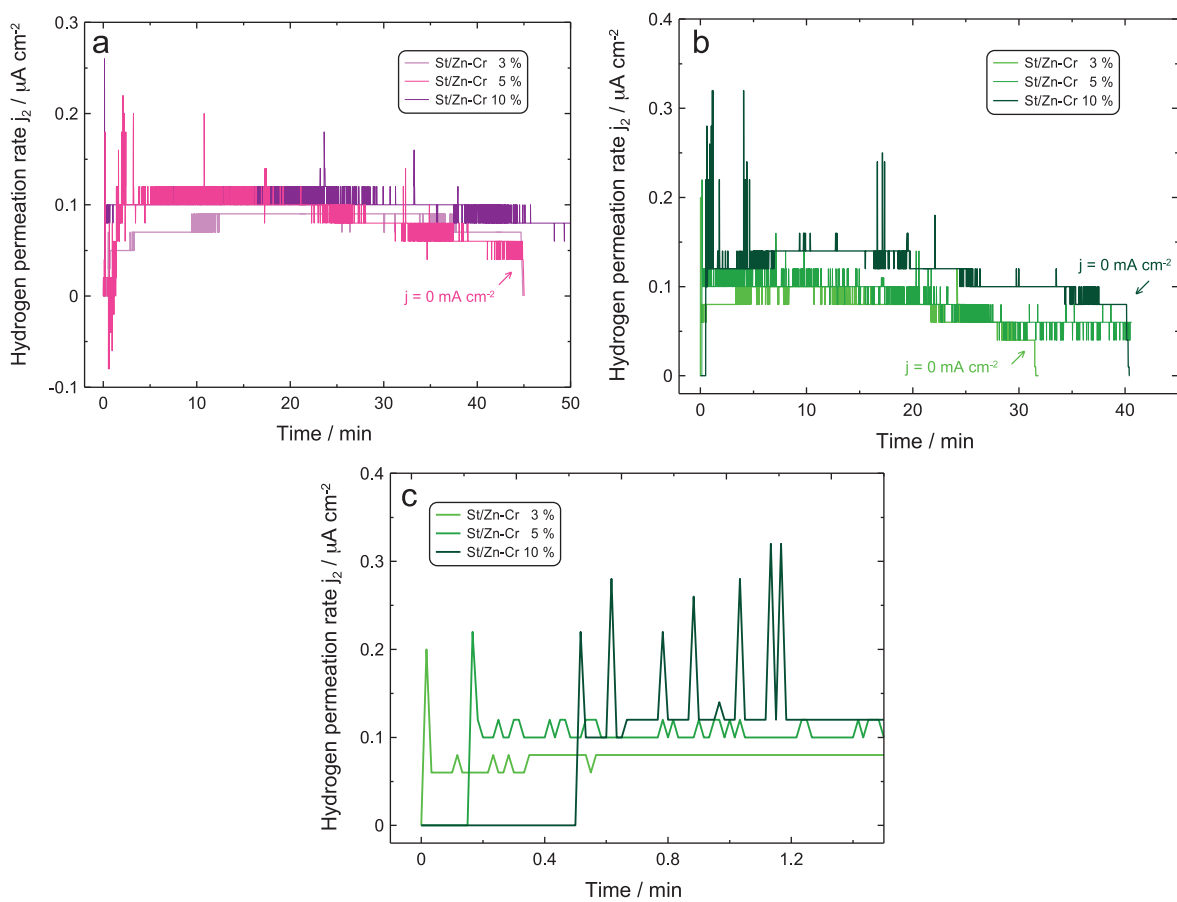


Fig. 8. Permeation transients, measured during polarization of St/Zn-Cr 2.5 μm (a) and St/Zn-Cr 5 μm (b and c) with 3, 5 or 10% Cr at $j_1 = 300 \text{ mA cm}^{-2}$ in 0.5 M Na_2SO_4 solution, pH 6 with different time resolution: 40 min (a and b) and 1.5 min (c).

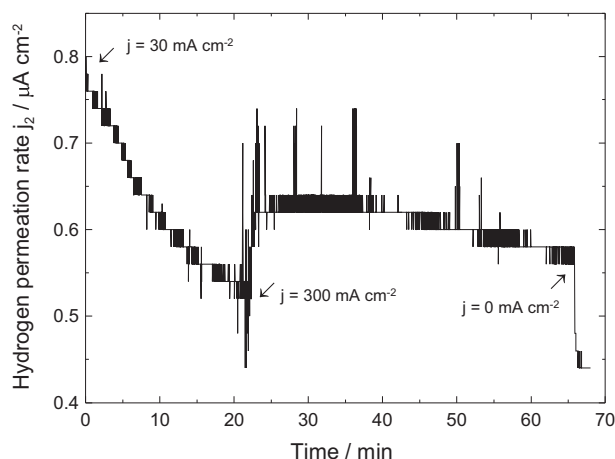


Fig. 9. Permeation transients, measured during subsequent polarization of St/Zn–Cr 10%, 2.5 μm at $j_1 = 30$ and 300 mA cm^{-2} in $0.5 \text{ M Na}_2\text{SO}_4$ solution, pH 6. (The curve in the figure starts from the residual anodic current density.)

The transients, corresponding to the different content of Cr in the Zn–Cr alloy coatings show a slight increase of the maximal and steady state permeation rate with the increase of Cr content from 3 to 10% at both thickness of the coatings (2.5 μm and 5 μm). Moreover, the comparison of the curves (particularly their beginning, well seen in Fig. 8c) reveals a tendency for increasing delay with the increase of the Cr content. This could be related to trapping of hydrogen within the alloy coatings. Furthermore, an increase of the frequency and the amplitude of the fluctuations of the permeation current with increasing the content of Cr in the Zn–Cr coatings is observed.

The comparison of the transients of St/Zn–Cr (Fig. 8) with that of the bare steel (Fig. 1b) reveals the strong inhibition effect of the Zn–Cr coatings on hydrogen penetration into the steel substrate even at the very high charging current density of 300 mA cm^{-2} .

The influence of the charging current on the hydrogen permeation characteristic in the case of St/Zn–Cr system is also evaluated. Fig. 9 shows the transients obtained with St/Zn–Cr 10%, 2.5 μm in one and the same experiment at a charging current density of 30 mA cm^{-2} and 300 mA cm^{-2} , respectively.

As in the case of St/Zn 2.5 μm , at the low charging current there is no indication for hydrogen permeation into the steel during 20 min. Rather, the flow of hydrogen from the substrate/coating system continues. As soon as a charging current of 300 mA cm^{-2} is applied, the hydrogen permeation rate is increased. The transient is characterized by numerous peaks, especially in the first minutes after polarization of the entry side of the sample as well as by an unstable steady state permeation rate. The low maximal and steady state permeation rates again confirm the barrier effect of the Zn–Cr coatings on the hydrogen penetration into the steel. However, the current fluctuations are an indication for irregular permeation of small amounts of hydrogen through the system.

The fluctuations of the permeation current are most probably due to the evolution of hydrogen bubbles from the electrode surface as a result of the cathode polarization and of course, as a result of the catalytic and bulk properties of the alloy coatings, regarding hydrogen evolution and permeation. During cathode hydrogen charging of Armko iron membrane, an excellent correlation between the fluctuations of the concentration of the absorbed hydrogen in the first layers of metal, the fluctuations of the cathode potential and the permeation current was found [19,20]. In the present study, performed at a considerably higher current density, no correlation between the fluctuations of the potential and the fluctuations of the permeation current was established.

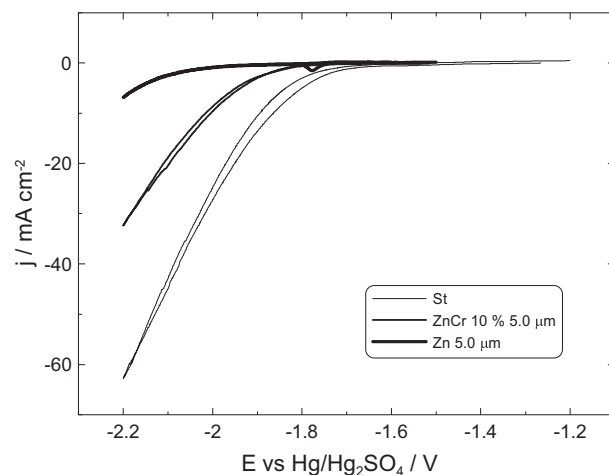


Fig. 10. Voltammograms obtained for St, Zn and Zn–Cr alloy coatings in $0.5 \text{ M Na}_2\text{SO}_4$ solution, pH 6.

Fig. 10 presents voltammograms on steel, Zn and Zn–Cr alloys. It is seen that the co-deposition of Cr alters the catalytic properties of Zn, facilitating the HER. However, the permeation current reflects both the surface (interface electrode/electrolyte) and the bulk properties (hydrogen transport through the systems). It seems that the bulk properties of the coatings tested determine the hydrogen permeability.

The insignificant influence of the Cr content in the Zn coating (Zn and Zn–Cr alloys) on the hydrogen diffusion flux could be explained by the similarity in the bulk properties of the Zn and the Zn–Cr alloys, electrocrystallizing in a hexagonal crystal structure. The alloy with 3 mass% Cr comprises of hcp η -(Zn,Cr) phase and the main constituent of the 10 mass% Cr alloy is the hcp δ -(Zn,Cr) phase. Both phases are solid solutions of Cr in the Zn matrix, formed by random substitution of Cr for Zn [21]. The increase of the Cr content in the alloy reflects in a change of the lattice parameters of the hexagonal phase.

The polarization of the Zn–Cr 10%, 2.5 μm at the higher charging current brings alteration of the surface of the coating (Fig. 11). Crystal agglomerates, with a chemical composition very close to that of the base coating, are observed on the top of the polycrystalline particles.

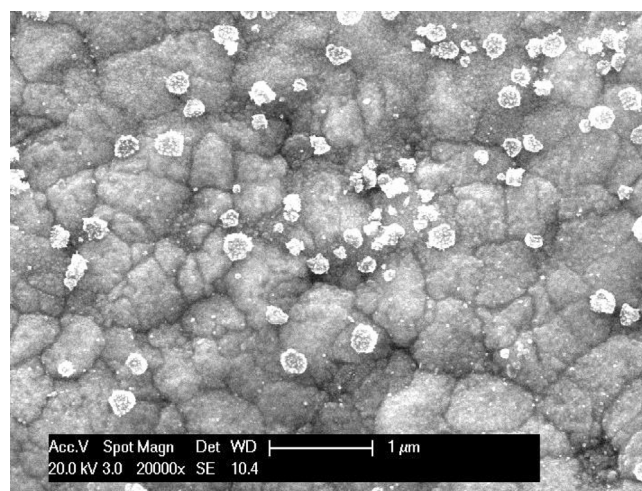


Fig. 11. SEM images of Zn–Cr 10%, 2.5 μm after polarization at $j_1 = 300 \text{ mA cm}^{-2}$ in $0.5 \text{ M Na}_2\text{SO}_4$ solution, pH 6.

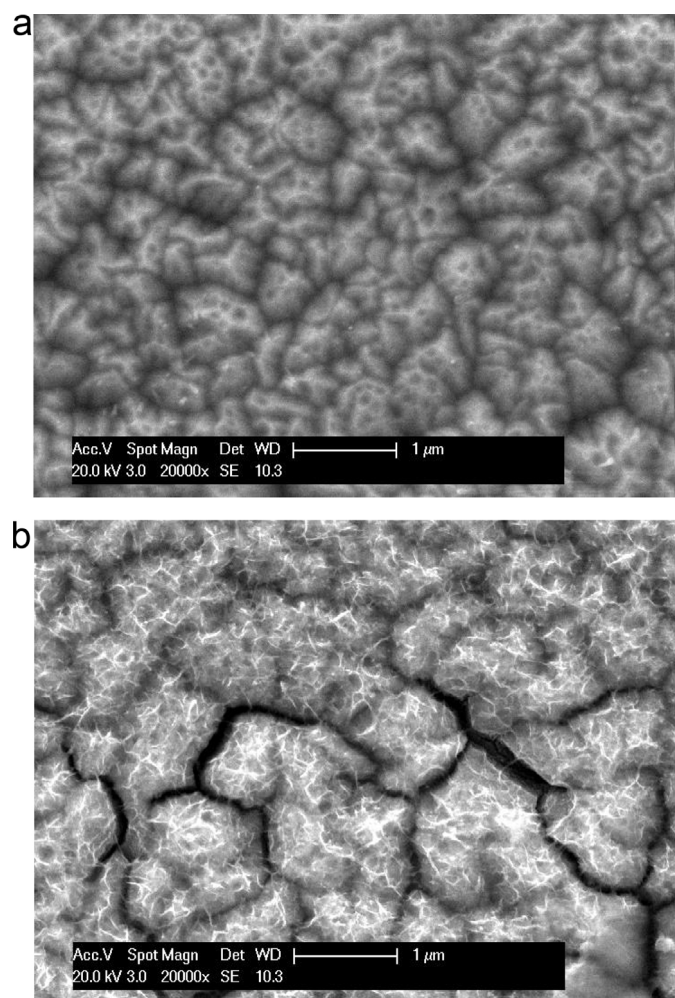


Fig. 12. SEM images of Zn–Cr 5%, 5 μm before (a) and after (b) polarization at $j_1 = 300 \text{ mA cm}^{-2}$ in 0.5 M Na_2SO_4 solution, pH 6.

The consequence of the charging of the coatings at the higher current on their structure is well expressed in the case of the 5 μm thick Zn–Cr 5% coatings (Fig. 12).

Due to the hydrogen impact, cracks at grain boundaries are formed, as it is demonstrated by the SEM images (Fig. 12b). This effect is stronger for the alloy coatings with higher Cr content.

3.4. Effect of the presence of oxygen in the solution on the hydrogen permeation during polarization of steel, electroplated with Zn or Zn–Cr coating

In order to evaluate the effect of oxygen in the electrolyte used for hydrogen permeation studies, experiments with St/Zn 2.5 μm and St/Zn–Cr 10%, 2.5 μm were performed after blowing Ar through the solution for 1 h. Comparative graphics (transients in aerated and de-aerated medium) for both systems are presented in Fig. 13.

The transients for both systems change significantly in de-aerated medium – the rate of hydrogen permeation is higher and the permeation current fluctuations show higher frequency and amplitude. Comparison of the transients of Zn 2.5 μm (Fig. 13a) and Zn–Cr 10%, 2.5 μm (Fig. 13b) systems in de-aerated medium shows considerably “stronger” fluctuations of the permeation current in the case of the Zn–Cr 10% system and a higher average rate of hydrogen permeation.

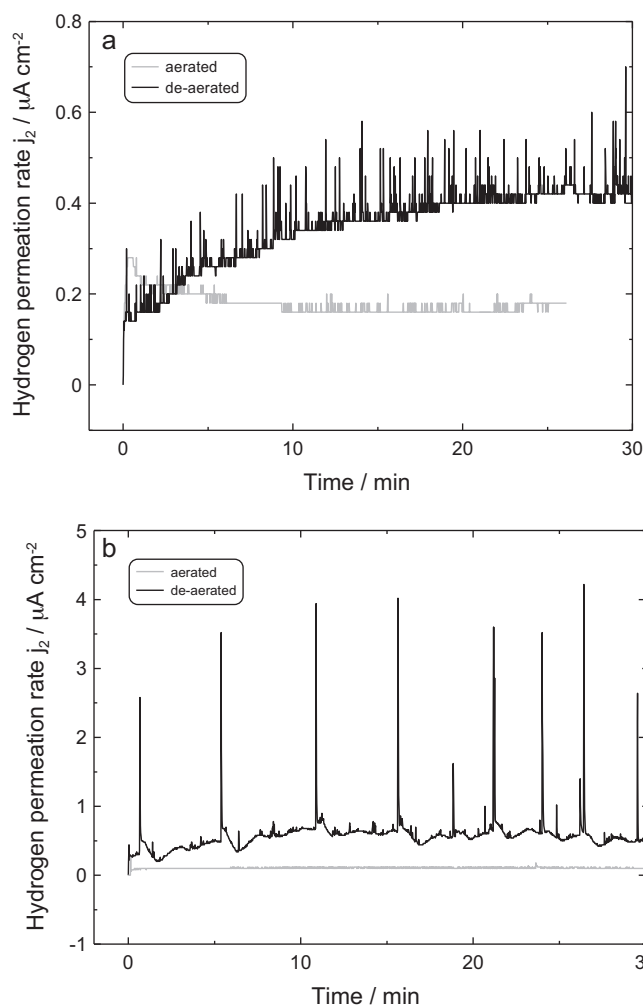


Fig. 13. Permeation transients measured during polarization of St/Zn 2.5 μm (a) and St/Zn–Cr 10%, 2.5 μm (b) at $j_1 = 300 \text{ mA cm}^{-2}$ in aerated and de-aerated 0.5 M Na_2SO_4 solution, pH 6.

The difference between the transients, measured in aerated and de-aerated solutions could be related to the surface state of the layers. The absence of oxygen in the de-aerated solution affects the oxidation state of the surface and respectively the level of its

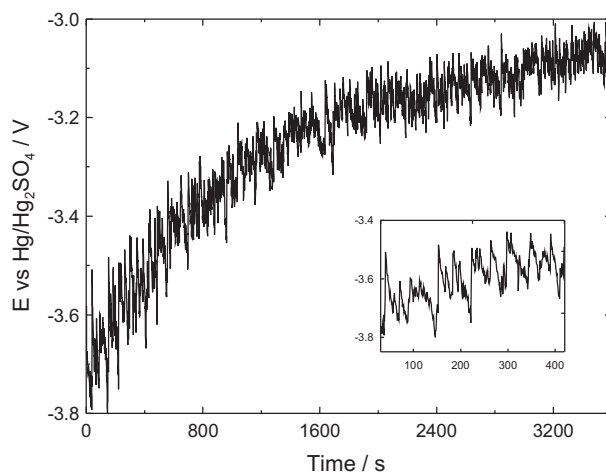


Fig. 14. Galvanostatic potential vs. time curve for Zn–Cr 10%, 2.5 μm in de-aerated 0.5 M Na_2SO_4 solution, pH 6 measured at a current density of 300 mA cm^{-2} .

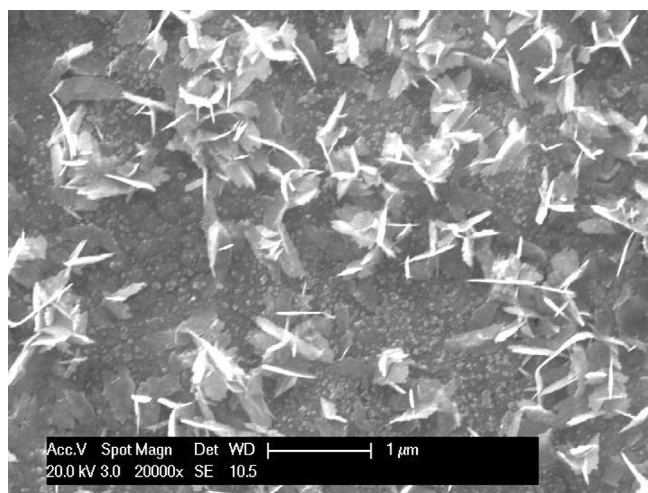


Fig. 15. SEM image of Zn–Cr 10%, 2.5 μm after polarization at $j_1 = 300 \text{ mA cm}^{-2}$ in de-aerated 0.5 M Na_2SO_4 solution, pH 6.

degradation. Higher surface coverage of the electrodes with atomic hydrogen, formed as a result of the cathode polarization, could also be supposed in the de-aerated solution.

In the de-aerated, as well as in the aerated media, the differences in the permeation currents for St/Zn and St/Zn–Cr systems are related to the catalytic properties of the Zn and Zn–Cr alloys towards the HER and mostly to the bulk properties of the layers, regarding hydrogen transport. It is important to mention, that the thermal desorption analysis showed hydrogen differently bound in the St/Zn–Cr system and higher values for the amount of hydrogen desorbed from the St/Zn–Cr system in comparison to St/Zn system.

The potential vs. time curve recorded in a de-aerated solution at a current density of 300 mA cm^{-2} (Fig. 14) demonstrates a frequency relationship, which however does not correspond to that of the fluctuations, registered in the permeation transients (Fig. 13b). Similar relationship was obtained for aerated solutions.

The SEM image in Fig. 15 represents the surface morphology, resulting from the polarization of Zn–Cr 10%, 2.5 μm coating (according to Fig. 13b) in the de-aerated solution.

4. Conclusions

On the basis of the results presented on Steel/Zn and Steel/Zn–Cr systems, subjected to hydrogen permeation measurements with the Zn or Zn–Cr coating at the entry side of the steel membrane the following conclusions could be drawn:

- The Zn and Zn–Cr coatings are impermeable during hydrogenation at a low charging current density of 30 mA cm^{-2} .
- They permeate small amounts of hydrogen when a high charging current density of 300 mA cm^{-2} is applied. However, the hydrogen amount permeating into the steel substrate is significantly lower as compared with that permeating into the bare steel. Therefore, Zn and Zn–Cr coatings play a role of an effective protection of the steel under conditions which cause hydrogen ingress.
- The hydrogen permeation through the Zn and Zn–Cr coatings is not a continuous process. Fluctuations of the permeation current, more expressed in the case of Steel/Zn–Cr system are registered. The alloying of Zn with Cr alters the catalytic properties of coatings, regarding the HER and the bulk properties, regarding hydrogen diffusivity and trapping effects. It seems that the bulk properties of the coatings determine the hydrogen permeability.

- In de-aerated medium the permeation current fluctuations have higher frequency and higher amplitude. This could be related to the different level of degradation of the surface, resulting from the absence of oxygen in the solution.
- The charging of the Zn or Zn–Cr coatings at a high current density of 300 mA cm^{-2} leads to lasting structural alterations – disintegration of a subsurface metal layer in the case of Zn and in addition, cracks formation in the case of Zn–Cr alloys.

The influence of the thickness of the Zn and Zn–Cr coatings as well as the influence of the Cr content in the Zn–Cr alloy on the hydrogenation of the steel substrate is expressed by negligible differences in the hydrogen permeation rates. Nevertheless, the following tendencies could be defined:

- The hydrogen permeation rate decreases with the increase of the thickness of the Zn or Zn–Cr coatings.
- The hydrogen permeation rate increases with the increase of the Cr content in the Zn–Cr alloy coatings.

Acknowledgement

These investigations have been performed with the support of the Austrian Science Foundation FFG and the government of Lower Austria in the frame of the COMET-program.

References

- [1] B. Chatterjee, *Electrodeposition of zinc alloys*, *Jahrbuch Oberflächentechnik* 62 (2006) 76.
- [2] T. Steck, J. Gerdenitsch, A. Tomandl, W. Achleitner, J. Faderl, T. Lavric, T. Boiadjieva-Scherzer, H. Kronberger, Zinc–chromium coated steel sheet: properties and production, in: 8th International Conference on Zinc and Zinc Alloy Coated Steel Sheet, IAM, 2011, p. 1133.
- [3] Tz. Boiadjieva, L. Mirkova, H. Kronberger, T. Steck, M. Monev, Hydrogen permeation in steel during electroplating of Zn and Zn–Cr coatings, *Journal of the Electrochemical Society* 159 (2012) D730.
- [4] W. Paatsch, Studies of hydrogen embrittlement of heat-treated steels during electroplating – 1. Hydrogen permeation tests, *Metalloberfläche* 32 (1978) 546.
- [5] M. Monev, L. Mirkova, I. Krastev, Hr. Tzvetkova, St. Rashkov, W. Richtering, Effect of brighteners on hydrogen evolution during zinc electroplating from zincate electrolytes, *Journal of Applied Electrochemistry* 28 (1998) 1107.
- [6] T. Casanova, F. Soto, M. Eyraud, J. Crousier, Hydrogen absorption during zinc plating on steel, *Corrosion Science* 39 (1997) 529.
- [7] A. El hajjami, M.P. Gigandet, M. De Petris-Wery, J.C. Catonne, J.J. Duprat, L. Thiery, F. Raulin, B. Starck, P. Remy, Hydrogen permeation inhibition by zinc–nickel alloy plating on steel XC68, *Journal of Applied Surface Science* 255 (2008) 1654.
- [8] W. Paatsch, R. Landgrebe, M.M. Lohrengel, Hydrogen embrittlement potentials on zinc and zinc–nickel coatings over high tensile steel, *Galvanotechnik* 100 (2009) 1280.
- [9] A. Durairajan, D.S. Slavkov, B.N. Popov, Development of corrosion and hydrogen permeation resistant Zn–Ni–X (X = P Cd) ternary alloy coatings, *Bulletin of the Chemists and Technologists of Macedonia* 20 (2001) 3.
- [10] H. Kim, B. Popov, K. Chen, Comparison of corrosion-resistance and hydrogen permeation properties of Zn–Ni, Zn–Ni–Cd and Cd coatings on low carbon steel, *Corrosion Science* 45 (2003) 1505.
- [11] E.M.K. Hiillier, M.J. Robinson, Permeation measurements to study hydrogen uptake by steel electroplated with zinc–cobalt alloys, *Corrosion Science* 48 (2006) 1019.
- [12] J.L. Cao, L.T. Li, J.X. Wu, Y.P. Lu, Z.L. Gui, Diffusion of hydrogen in steel substrate absorbed during zinc and zinc–silica electroplating, *Corrosion* 58 (2002) 698.
- [13] M.A.V. Devanathan, L. Stachurski, The adsorption and diffusion of electrolytic hydrogen in palladium, *Proceedings of the Royal Society (London) A* 270 (1962) 90.
- [14] Tz. Boiadjieva, D. Kovacheva, K. Petrov, S. Hardcastle, A. Sklyarov, M. Monev, Electrodeposition, composition and structure of Zn–Cr alloys, *Journal of Applied Electrochemistry* 34 (2004) 315.
- [15] T. Zaczoczynski, Z. Szklarska-Smialowska, Activation of iron surface to hydrogen absorption resulting from a long cathodic treatment in NaOH solution, *Journal of the Electrochemical Society* 132 (1985) 2548.
- [16] T. Zaczoczynski, Adaptation of the electrochemical permeation technique for studying entry, transport and trapping of hydrogen in metals, *Electrochimica Acta* 51 (2006) 2261.
- [17] T. Zaczoczynski, N. Lukomski, J. Flis, Entry and transport of hydrogen in ion nitrated iron, *Journal of the Electrochemical Society* 140 (1993) 3578.

- [18] N.N. Tomashova, Cathodic incorporation of alkali metals and alteration of the electrode properties, in: 7th Frumkin Symposium on Electrochemistry, Basic Electrochemistry for Science and Technology, Moscow, October 23–28, Proceedings Part II, 2000, p. 556.
- [19] F. Huet, M. Jerome, P. Manolatos, F. Wenger, Influence of hydrogen absorption on the electrochemical potential noise of an iron electrode under corrosion with gas evolution, in: J.R. Kearns, et al. (Eds.), *Electrochemical Noise Measurement for Corrosion Applications*, ASTM STP 1277, 1996, p. 375.
- [20] Z. Amrani, F. Huet, M. Jerome, P. Manolatos, F. Wenger, Fluctuations of permeation rate through an iron membrane induced by hydrogen bubbles, *Journal of the Electrochemical Society* 141 (1994) 2059.
- [21] Tz. Boiadjieva, K. Petrov, H. Kronberger, A. Tomandl, G. Avdeev, W. Artner, T. Lavric, M. Monev, Composition of electrodeposited Zn–Cr alloy coatings and phase transformations induced by thermal treatment, *Journal of Alloys and Compounds* 480 (2009) 259.